Duc Duong-Hong[1,2]
Jongyoon Han[2,3,4]*
Jian-Sheng Wang[2,5]
Nicolas G. Hadjiconstantinou[2,6]
Yu Zong Chen[2,7]
Gui-Rong Liu[2,8]

[1]Abbott Vascular, Santa Clara, CA, USA
[2]Singapore – MIT Alliance, Singapore, Singapore
[3]Department of Electrical Engineering and Computer Science, Massachusetts Institute of Technology, Cambridge, MA, USA
[4]Department of Biological Engineering, Massachusetts Institute of Technology, Cambridge, MA, USA
[5]Department of Physics, National University of Singapore, Singapore
[6]Department of Mechanical Engineering, Massachusetts Institute of Technology, Cambridge, MA, USA
[7]Department of Pharmacy, National University of Singapore, Singapore
[8]Department of Mechanical Engineering, National University of Singapore, Singapore

Received April 21, 2008
Revised June 30, 2008
Accepted July 3, 2008

Research Article

Realistic simulations of combined DNA electrophoretic flow and EOF in nano-fluidic devices

We present a three-dimensional dissipative particle dynamics model of DNA electrophoretic flow that captures both DNA stochastic motion and hydrodynamics without requiring expensive molecular dynamics calculations. This model enables us to efficiently and simultaneously simulate DNA electrophoretic flow and local EOF (generated by counterions near the DNA backbone), in mesoscale (∼μm) fluidic devices. Our model is used to study the electrophoretic separation of long DNA chains under entropic trapping conditions [Han and Craighead, *Science* 2000, *288*, 1026–1029]. Our simulation results are in good agreement with experimental data for realistic geometries (tapered walls) and reveal that wall tapering in entropic traps has a profound impact in the DNA trapping behavior, an effect which was largely ignored in previous modeling.

Keywords:
Debye layer / Dissipative particle dynamics method / DNA separation / Entropic trapping / Microfluidics
DOI 10.1002/elps.200800257

1 Introduction

Statics and dynamics of polyelectrolytes have been studied for a long time because of their relevance to many important applications such as oil extraction from porous rock and DNA separation for sequencing [1, 2]. Of particular interest is the problem of DNA (model polyelectrolyte) interacting with device boundaries under the action of an electric field, which affects both the DNA's mobility and conformation. During the last 10 years, there has been an explosion of both experimental and theoretical studies on this subject, largely with the intention of developing new tools for genomics.

Unfortunately, the current status of computational modeling for this particular problem falls far short of providing truly predictive models for polyelectrolyte dynamics. Current models fail to consider various factors involved in the electrophoresis of polyelectrolytes, such as the local EOF generated by the counterion clouds surrounding the molecule. When a polyelectrolyte is acted upon by a non-electric force (for example, held by an optical trap or a micropillar in a microchannel), counterions generate a local EOF [1, 3], which complicates the hydrodynamics of the problem. Since other polymer dynamical properties such as (Zimm) diffusivity critically depend on the local fluid flow, accurate prediction of polymer behavior requires the inclusion of this local EOF in the model. The work presented in this paper addresses this deficiency by proposing a method for capturing the local EOF in dissipative particle dynamics (DPD) simulations thus allowing, for the first time, efficient (mesoscopic rather than microscopic) simulation of DNA electrophoretic flow under the action of an electric field in a nanoscale device. The particular device chosen here is the one from the experiments of

Correspondence: Dr. Duc Duong-Hong, Abbott Vascular, 3200 Lakeside Drive, Santa Clara, CA 95054, USA
E-mail: duc.duong@av.abbott.com
Fax: +1-408-845-4258

Abbreviations: DPD, dissipative particle dynamics; **LF,** local-flow

*Additional corresponding author: Associate Professor Jongyoon Han, E-mail: jyhan@MIT.EDU

Han and coworkers (described in Fig.1) to allow for direct comparison between our simulations and experiments. The latter are representative of a large volume of recent research work on biomolecule separation devices.

Han and coworkers [4–6] have fabricated microchannels consisting of periodically alternating deep and shallow regions (T-channel in short) as depicted in Fig. 1 (so-called entropic trapping). Soon after this behavior was explained by transition state theory [4], a series of numerical investigations of this phenomenon appeared, including Monte Carlo simulations [7, 8] and Brownian Dynamics [9, 10] simulations. However, in these simulations, like all other simulations reported previously, the solvent flow was not explicitly modeled, and therefore, the EOF and hydrodynamic interactions were both neglected, making it difficult to capture the interplay between sieving and diffusion/dispersion in the device, which is essential for correctly predicting DNA behavior and optimizing the device performance. Modeling such behavior would require inclusion of Debye screening layer charges on the DNA backbone, which is quite challenging and has not been done to date. Strictly speaking, without such an effect explicitly included in the model, one cannot reproduce the free-draining behavior – one of the most basic properties in DNA electrophoresis – correctly. We would also like to remark that although the free-draining behavior of DNA electrophoresis often allows one to omit the hydrodynamic interaction, the resulting diffusion behavior and interactions with the wall which are mechanical in nature, may affect the overall system behavior [3].

In this paper, we present a DPD model that reproduces the free-draining mobility of DNA under electrophoretic conditions, making this the first time, to the best of our knowledge, that both electrophoretic flow and EOF are simultaneously modeled in a simulation. The DNA model is validated by measuring its diffusion coefficient and its free-draining mobility for various DNA chain lengths. In the latter part of the paper, we use our model to study the electrophoretic mobility in practical geometries such as the one shown in Fig. 1, and show that tapered walls in entropic traps have a significant impact on the separation efficiency of the device. By taking the tapering angle α into account, we can reproduce experimental results very well, and show that neglecting wall taper (*i.e.* taking $\alpha = 0^\circ$, as in most previous modeling) results in overestimated trapping effects. Finally, we comment on the effects of EOF.

2 A brief description of the DPD method

DPD has been first introduced by Hoogerbrugge and Koelman [11] for studying the hydrodynamic behavior of complex fluids. The method has been successfully applied for various complex systems such as DNA suspensions [12], multi-phase fluids [13], microfluidic systems [14], to name a few. The DPD method is based on a representation of materials by ensembles of particles. Every particle is defined by its position, velocity and mass. Based on Newton's equation of motion, the time evolution of the positions and velocities of DPD particles are calculated by,

$$\frac{\mathrm{d}\mathbf{r}_i}{\mathrm{d}t} = \mathbf{v}_i, \quad \frac{\mathrm{d}\mathbf{v}_i}{\mathrm{d}t} = \sum_{j \neq i} \mathbf{f}_{ij} + \mathbf{F}_\mathrm{e} \tag{1}$$

Here, we assume the mass of particles to be identical and normalized to 1, $\mathbf{r}_i$ and $\mathbf{v}_i$ are the position and the velocity vectors of particle i, $\mathbf{F}_\mathrm{e}$ is the external force on the particle, and $\mathbf{f}_{ij}$ is the interparticle force (exerted on particle i by particle j), consisting of three parts:

$$\mathbf{f}_{ij} = \mathbf{F}_{ij}^\mathrm{C} + \mathbf{F}_{ij}^\mathrm{D} + \mathbf{F}_{ij}^\mathrm{R} \tag{2}$$

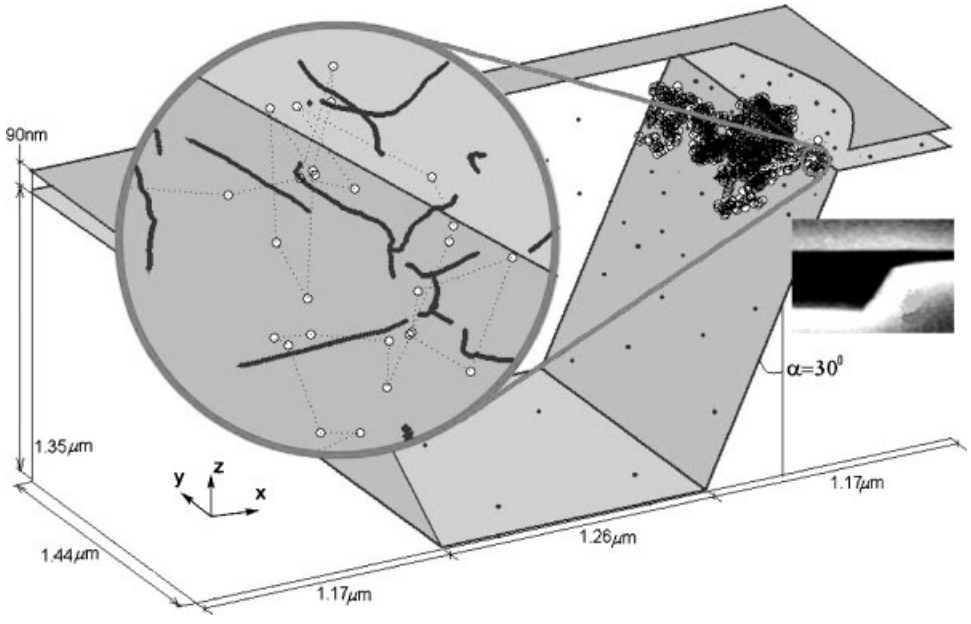

Figure 1. The geometry of T-channel; the DNA chain entering the nano-slit of T-channel is shown. The inset (right) shows a picture of the experimental channel (reproduced from Ref. [6]). The zoomed picture (left) shows paths of solvent particles (blue dots) during one DPD unit time in the vicinity of DNA segment (open round connected by dotted lines).

The conservative force, $\mathbf{F}_{ij}^{C}$, is given by

$$\mathbf{F}_{ij}^{C} = \begin{cases} a_{ij}(1 - r_{ij}/r_c)\hat{\mathbf{r}}_{ij}, & (r_{ij} < r_c) \\ 0, & (r_{ij} \geq r_c) \end{cases} \quad (3)$$

where a_{ij} is the maximum repulsion between particles i and j, $\mathbf{r}_{ij} = \mathbf{r}_i - \mathbf{r}_j$, $r_{ij} = |\mathbf{r}_{ij}|$, $\hat{\mathbf{r}}_{ij} = \mathbf{r}_{ij}/r_{ij}$ is the unit vector directed from particle j to i, and r_c is a cut-off radius, here normalized to unity.

The dissipative force, $\mathbf{F}_{ij}^{D}$, and the random force, $\mathbf{F}_{ij}^{R}$, are given by

$$\mathbf{F}_{ij}^{D} = -\gamma\omega^{D}(r_{ij})(\hat{\mathbf{r}}_{ij} \cdot \mathbf{v}_{ij})\hat{\mathbf{r}}_{ij} \quad (4)$$

and

$$\mathbf{F}_{ij}^{R} = \sigma\omega^{R}(r_{ij})\theta_{ij}\hat{\mathbf{r}}_{ij} \quad (5)$$

respectively, where $\mathbf{v}_{ij} = \mathbf{v}_i - \mathbf{v}_j$, and γ and σ are the coefficients characterizing the strengths of the dissipative and random forces, ω^{D} and ω^{R} are the weight functions that vanish if $r \geqslant r_c$, and θ_{ij} is a white noise with the properties:

$$\langle\theta_{ij}(t)\rangle = 0 \text{ and } \langle\theta_{ij}(t)\theta_{kl}(t')\rangle = (\delta_{ik}\delta_{jl} + \delta_{il}\delta_{jk})\delta(t - t') \quad (6)$$

To satisfy detailed balance [15], the weight functions obey a relation similar to the fluctuation-dissipation theorem

$$\omega^{D}(r) = [\omega^{R}(r)]^2 \text{ and } \gamma = \frac{\sigma^2}{2k_B T} \quad (7)$$

where $k_B T$ is the Boltzmann temperature. The weight function is calculated by,

$$\omega^{D}(r) = [\omega^{R}(r)]^2 = \begin{cases} \sqrt{1 - r/r_c} & r < r_c \\ 0 & r \geq r_c \end{cases} \quad (8)$$

The equations of motion (1–8) are solved by using the Velocity-Verlet algorithm suggested by Groot and Warren [16]. Note that in DPD, macroscopic quantities such as density and linear momentum satisfy the conservation laws of continuum mechanics; this makes DPD attractive, and has led some to consider it as a statistical method for solving continuum mechanics problems.

Unless otherwise stated, standard DPD methods [11, 14–17] are used for our simulations. The density of solvent is chosen to be 0.1, and the cut-off radius, r_c, is set to 2.0. (This condition agrees with the typical condition $\rho_{DPD} \sim r_c^{-3}$, so that the DPD solvent still presents a fluid phase [16]. The compressibility of the solvent is also calculated through the procedure suggested by Groot and Warren [16]; our calculations yield a value of 14.5, which is comparable with that of water, *i.e.* ~16. Finally, the viscosity of DPD fluid is measured using Couette flows and its value is comparable with that of water at room temperature.) Other DPD parameters for solvent particles are given in Refs. [14–17] and listed in Table 1. Our parameter choices give an energy unit $[\varepsilon] = k_B T = 4.14 \times 10^{-21}$ J, for $T = 300$ K, a length scale $[\sigma] = 18$ nm and a mass unit $[m] = 2 \times 10^{-14}$ kg. The time scale $[t]$ is then calculated as $\sqrt{m^2/\epsilon} \approx 3.95 \times 10^{-5}$ s. Each time step, Δt, is $0.01[t]$~0.395 μs. Typical run lengths were between 5×10^6 and 2×10^7 time steps corresponding to about 2–8 s.

Table 1. DPD parameters

DPD parameters	Value
$k_B T$	1
a_{ij} (fluid–fluid)	375
a_{ij} (chain–chain)	10
a_{ij} (fluid–chain)	1
a_{ij} (fluid–wall or chain–wall)	12.75
σ (fluid–fluid or chain–chain)	3
σ (fluid–chain)	0.5

3 DNA model and simulation results

The polymer chain is modeled by a number of DPD particles, which are connected by springs [12, 18]. Recently, several DPD models for simulating λ-DNA molecules have been suggested [12, 18]. However, their length scale, typically of the order of 1 μm, is too large to apply in our systems, which feature dimensions as small as 90 nm (see Fig. 1).

The springs in our model derive from a ''worm-like'' model [12, 18–20],

$$\mathbf{F}_{ij}^{W} = -\frac{k_B T}{4P}\left[\left(1 - \frac{r_{ij}}{l}\right)^{-2} + \frac{4r_{ij}}{l} - 1\right]\hat{\mathbf{r}}_{ij} \quad (9)$$

where r_{ij} is the distance between beads i and j, l is the maximum length of one chain segment, and P is the effective persistence length, here given the value $P = 50$ nm as is typical in the literature [21]. We choose the maximum segment length to be $2.778[\sigma]$ leading to a correspondence of 80, 240, 360, and 800 bead chains for DNAs of 11.61, 35.14, 52.79, and 117.5 kbp, respectively.

EOF caused by the wall surface charges is included in our simulations (where applicable) using a recently developed method [14], valid in the limit of thin Debye layer. In this method, the velocity of wall particles is set equal to the velocity of the mobile ion-layer in the Debye layer at the same position; by using a no-slip boundary condition [17], the EOF is eventually established through the action of viscosity [14]. This method can be applied effectively for both simple and complex channel geometries.

Our baseline DNA model is first validated by comparing the diffusion coefficient of DNA chains with other experimental data. Note that, for these tests, the DNA chains are suspended in a sea of solvent while periodic boundary conditions are applied in all directions, and that DNA and solvent particles are both neutral. The numerical results shown in the inset of Fig. 2 are in very good agreement with Stellwagen's formula [22] and Nkodo's experimental data [21], where the slopes of diffusion coefficient are reported to be −0.67 and −0.57, respectively. Those values are in reasonable agreement with Zimm's scaling [21], *i.e.* −0.60.

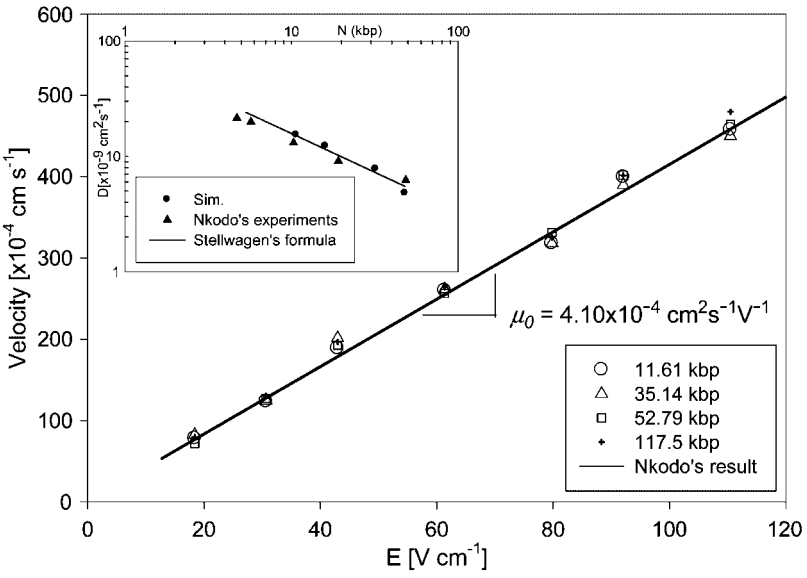

Figure 2. A comparison of the diffusion coefficient and free-draining mobilities of different DNA chains and experimental results of Nkodo *et al.* [21], $\mu_0 = (4.1 \pm 0.4) \times 10^{-4}\,\mathrm{cm^2\,s^{-1}\,V^{-1}}$.

3.1 The local-flow effect

We now discuss our model of hydrodynamic and electrostatic interactions within the Debye layer, which makes our DPD model capable of capturing the DNA free-draining mobility. In DNA electrophoresis, electrostatic interactions and the resulting fluid shearing mainly occur within the Debye layer, which under the conditions considered here is very thin. As a result of these screening processes [3], the DNA electrophoretic mobility becomes independent of the strand contour length. Accurate modeling of this phenomenon requires explicit modeling of counterion charges, which is difficult and prohibitively expensive. (In fact, none of the previous modeling attempts considered this phenomenon.) To circumvent this limitation, we propose below a DPD-based technique that mimics the behavior of DNA and solvent particles in free-draining situations. The essence of this technique, which we will refer to as the local-flow (LF) effect, is the following: when the distance between a fluid particle and a DNA segment becomes smaller than the Debye length (due to the ''soft'' repulsive force-in DPD, a linear repulsive force is usually used rather than a power-law one like the Lennard-Jones function in molecular dynamics-between DPD particles, the particles are able to approach closely one another) the fluid particle acquires a counter-charge and it is thus driven to the cathode (if an electric field is present). Electrostatic interactions between the solvent and DNA particles are not taken into account.

Determining the solvent particle charge is difficult, especially since significant charge screening takes place within the Debye layer. As a first attempt, we assume that the fluid particle approaching the DNA chain within a Debye length possesses a positive charge equal to the value of the DNA-bead charge (as determined by the DNA effective charge that is discussed later). The fluid particle is then subject to an electric force that is equal to the one exerted on DNA particles, but in the opposite direction. As a result, one can effectively simulate the local EOF generated by the counterions around the DNA molecules, which is expected to create significant flow around the molecule when the DNA molecule is trapped in the entropic barrier. While this local EOF is technically similar to the EOF caused by charges on the device wall, we have chosen to use the above-mentioned technique instead of simply assigning a ''zeta-potential'' on the DNA backbone as in our previous publication [14]. Such treatment would work only for EOF generated by a flat, fixed surface, but not for fluctuating DNA molecules. This is mainly because the electrokinetic slip velocity around the molecule would become quite complicated when the size of the molecule (radius of the DNA backbone) becomes comparable to the size of the Debye layer. In addition, DNA conformation is expected to have an impact on the local EOF, which would complicate the simple ''molecular zeta-potential'' treatment.

Figure 3 demonstrates that the inclusion of the LF effect produces a discernible difference in the EOF flow profile; in particular, we see that if the LF effect is on, the EOF profile is unperturbed (see part A of Fig. 3). The contrast between the two cases is more clearly demonstrated in part B (LF effect on) and part C (LF effect off) of the same figure. The figure shows that the free-draining model works well for molecules moving only under the influence of electric force where DNA electrophoresis will not create any fluid motion in the surrounding area, therefore rendering the DNA ''transparent'' to the fluid. In other words, this model allows us to include an approximation of the complex solvent–DNA interactions to effectively model the free-draining flow without compromising the computational efficiency of the method.

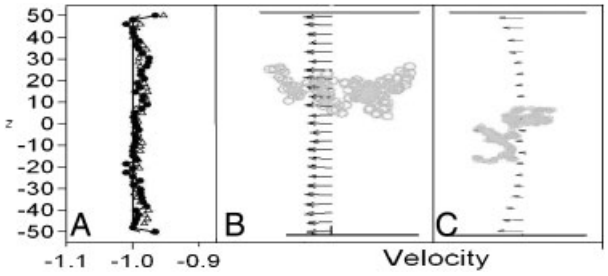

Figure 3. (A) Comparison of the normalized EOF velocity profile with the LF effect on in the presence (closed symbols) and absence (open symbols) of a DNA molecule. The solid line shows the Navier–Stokes solution. The data are averaged in 50 bins along the *z* direction over 200 time units and normalized by the theoretical EOF velocity. The velocity profile of local EOF in the vicinity of the DNA molecule in a free-draining flow when the LF effect is turned on (B), and when the LF effect is turned off (C). Data are sampled in 25 bins within a vicinity of DNA in one unit time.

For further validation of the model, the free-draining mobility of various DNA chains (μ_0) is computed over an electric field range of 20–120 V/cm at similar ionic concentration to the experiments of Nkodo, *i.e.* $C = 0.01$ M TBE [21]. The chains are separately placed in a large channel (dimensions of $500[\sigma] \times 100[\sigma] \times 100[\sigma]$ in x, y, and z directions, respectively), which is confined in the z direction and periodic boundary conditions are applied in both x and y directions. The results for different DNA chains are shown in Fig. 2; μ_0 can be clearly seen to be independent of DNA length and in excellent agreement with experimental results [21]. Assuming that the electric charge is uniformly distributed along each DNA segment, the effective charge of a DNA base pair is then computed to be 0.02e which is close to the value of 0.06e reported by Smith and Bendich [23].

4 Application to tapered-wall channels

Our model is then applied to the DNA separation problem in a T-channel that resembles the one used in Han's experiments [4]. Note that due to limitations of current lithography techniques, the ''vertical'' walls of the deep channel are in fact tapered (see the inset of Fig. 1). We denote the resulting tapering angle by α. We found that most of the previous simulation results [7–10] predict higher separation efficiencies (for the same resolution) than found in experiments [4]. Because we expected the tapering to have a measurable effect, two different channels were investigated: one is similar to the fabricated channel where $\alpha = 30^\circ$; it is denoted by Tp; and the other is an ''ideal channel'' usually studied in the literature with $\alpha = 0^\circ$ and denoted by Ti. Dimensions are shown in Fig. 1. In both simulations, the electric forces acting on each DNA bead are determined by a pre-computed solution for the electric field. (Specifically, given a potential difference V_0 due to the driving electric field, the distribution of the electric potential in the channel can be calculated by solving the Laplace equation with Neumann boundary conditions at the walls, assuming that the walls are perfect insulators). To minimize the computational cost, this solution is pre-computed and tabulated in the form of cell-averaged electric potential using a very fine grid of cells.

In order to compare our separation results with the experimental data of Han *et al.* [3] we carried out simulations at $C = 5\times$ TBE for two DNA chains modeled by 240 and 800 beads in Tp- and Ti-channels. (The mobility of two DNA chains of 35.14 and 107.4 kbp was investigated for electric fields in the range 35–120 V/cm for different ionic concentrations. We found that at the lower buffer concentration, *i.e.* 0.01 M TBE, the electroosmosis is so strong that it sweeps the DNA chains down the electroosmotic direction. This is consistent with observations of Han *et al.* [4] who used a high ionic concentration ($C = 5\times$ TBE$\sim$0.45 M TBE) to significantly reduce the effect of electroosmosis). In these simulations we used an effective charge of 0.012e *per* base pair. This was determined by Long's scaling [24] (mobility decreases by 10% when ionic strength doubles) because, unfortunately, no experimental data for μ_0 exist for the conditions in Han's experiments. The maximum mobility of DNA chain in our simulations is higher than that of experimental data. This suggests that the free-draining mobility in Han's experiments is lower than typical values in the literature [9]. Hence, for a consistent comparison, the experimental and simulation mobilities of DNA molecules are normalized by the $\mu_{\max}$ and plotted in Fig. 4.

The normalized mobilities of DNA chains in the Tp-channel are in good agreement with the experimental data of Han *et al.* and clearly show that the mobility of the longer chain is larger than that of the shorter DNA, particularly in the electric field range 35–55 V/cm. However, from our simulations we found that the separation efficiency of the ideal Ti-channel ($\alpha = 0^\circ$) in general is much higher than that of a tapered channel Tp ($\alpha = 30^\circ$) (supplementary video for the two cases is available). It is apparent that the inclined wall reduces the entropic barrier of the T-channel, and hence reduces the separating performance. Streek *et al.* [9] have observed that the DNA molecules spend more time at the side and the low corner of the deep channel. It follows that the escaping time is dependent on the diffusion of chains, which is, in turn, inversely proportional to the chain length. (Note that their simulation used the ideal Ti-channel where $\alpha = 0^\circ$.) We also sometimes observed DNA molecules ''tumbling'' along the vertical wall before escaping into the nano-slit of the Ti-channel. However, this is not observed in the Tp-channel since the inclined wall strongly supports the molecule at the entrance of the narrow region. Hence, the effect of DNA diffusion is strongly reduced in this case and, as a result, the separating performance is decreased. To fully assess the effect of wall tapering we simulated different degrees of tapering,

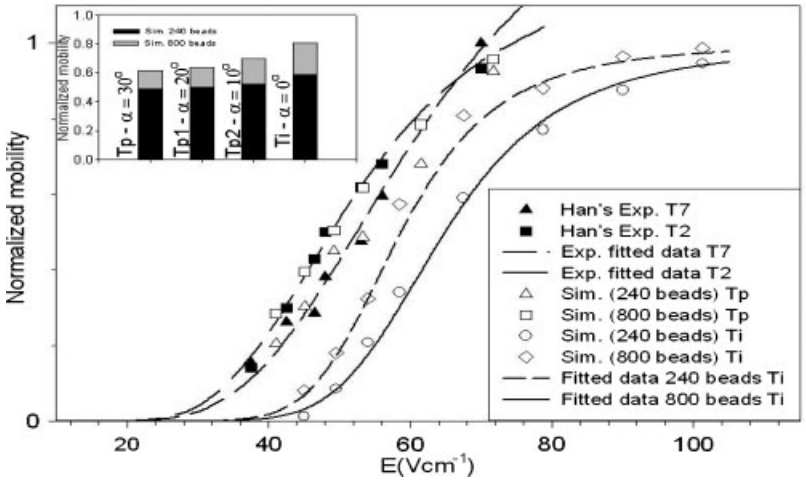

Figure 4. A comparison of the normalized mobilities of DNA chains in Tp-channels and Han's experimental data. The inset shows that the separating performance is improved as the tapering angle decreases. The data are well fitted by the equation

$$\mu = \mu_{max}/[1 + \alpha_1 \exp(\alpha_2/E)] \quad (10)$$

(curves) suggested by Han *et al.* [4]. The value of μ_{max} is that of μ at high field.

i.e. $\alpha = 10^\circ$ and 20°. The maximum separation observed for two chains of 35.14 and 117.5 kbp is plotted in the inset of Fig. 4. We found that at $\alpha = 20^\circ$ the separation performance is not improved significantly, but at $\alpha = 10^\circ$ the difference is more profound leading to a performance that is quite close to that of the ideal Ti-channel.

Some effects of the EOF on the DNA's behavior in the T-channel have also been observed. Before escaping, the DNA spends significant time at the entrance of the shallow channel, particularly for small tapering angle ($\alpha < 10^\circ$). The effect of EOF here is very strong, especially at low field. The inset in Fig. 1 shows some solvent particles passing through DNA segments when the DNA is trying to enter into the nano-slit. In the Ti-channel or Tp-channel with $\alpha = 10^\circ$, at low fields, DNA chains are observed to be pushed back to the well several times while trying to escape.

5 Conclusions

In conclusion, we have introduced a realistic DNA electrophoresis model based on the DPD method. The model is able to simulate coupled DNA electroosmotic and electrophoretic motion in micro- and nano-fluidic devices efficiently. This approach is one further step toward realistic simulation of experimental conditions. This work has shown that the free-draining mobility of DNA can be captured without including expensive electrostatic interactions. We also show that computed DNA mobilities in realistic geometries (Tp-channel – tapered walls) in general are in good agreement with the experimental data and that the separating performance of Ti-channel (non-tapered walls) is much larger than that of Tp-channel. Although DPD is a mesoscopic technique, complex systems such as the one studied here require significant computational resources (typical calculations take a few days on single-processor computers) especially if low-noise results are required. The model described here can be further used to investigate other effects of geometry (*i.e.* height ratios, channel lengths).

This study was funded by Singapore – MIT Alliance (SMA-II, Computational Engineering Program).

The authors have declared no conflict of interest.

6 References

[1] Viovy, J. L., *Rev. Mod. Phys.* 2000, *72*, 813–872.

[2] Slater, G. W., Guilouzic, S., Gauthier, M. G., Mercier, J.-F. *et al.*, *Electrophoresis* 2002, *23*, 3791–3816.

[3] Long, D., Viovy, J. L., Ajdari, A., *Phys. Rev. Lett.* 1996, *76*, 3858–3861.

[4] Han, J., Turner, H. G., *Phys. Rev. Lett.* 1999, *83*, 1688–1691.

[5] Han, J., Craighead, H. G., *Science* 2000, *288*, 1026–1029.

[6] Fu, P., Yoo, J., Han, J., *Phys. Rev. Lett.* 2006, *97*, 018103: 1–4.

[7] Tessier, F., Labrie, J., Slater, G. W., *Macromolecules* 2002, *35*, 4791–4800.

[8] Chen, Z., Escobedo, F. A., *Mol. Sim.* 2003, *29*, 417–425.

[9] Streek, M., Schmid, F., Duong, T. T., Ros, A., *J. Biotechnol.* 2004, *112*, 79–89.

[10] Panwar, A. S., Kumar, S., *Macromolecules* 2006, *39*, 1279–1289.

[11] Hoogerbrugge, P. J., Koelman, J. M. V. A., *Europhys. Lett.* 1992, *19*(3), 155–160.

[12] Fan, X-J., Phan-Thien, N., Chen, S., Wu, X., Ng, T., *Phys. Fluids* 2006, *18*, 063102: 1–10.

[13] Coveney, P. V., Español, P., *J. Phys. A: Maths Gen.* 1997, *30*, 779–784.

[14] Duong-Hong, D., Wang, J-S., Liu, G-R., Chen, Y. Z. *et al.*, *Microfluid. Nanofluid.* 2008, *4*, 219–225.

[15] Español, P., Warren, P., *Europhys. Lett.* 1995, *30*, 191–196.

[16] Groot, R. D., Warren, P. B., *J. Chem. Phys.* 1997, *107*, 4423–4435.

[17] Duong-Hong, D., Phan-Thien, N., Fan, X.-J., *Comput. Mech.* 2004, *35*, 24–29.

[18] Symeonidis, V., Karniadakis, G. E., Caswell, B., *Bull. Pol. Ac.: Tech.* 2005, *53*, 395–403.

[19] Shaqfeh, E. S. G., *J. Non-Newtonian Fluid Mech.* 2005, *130*, 1–28.

[20] Marko, J. F., Siggia, E. D., *Macromolecules* 1995, *28*, 8759–8770.

[21] Nkodo, A. E., Garnier, J. M., Tinland, B., Ren, H. *et al*., *Electrophoresis* 2001, *22*, 2424–2432.

[22] Stellwagen, E., Lu, Y., Stellwagen, N. C., *Biochemistry* 2003, *42*, 11745–11750.

[23] Smith, S. B., Bendich, A. J., *Biopolymers* 1990, *29*, 1167–1173.

[24] Long, D., Viovy, J. L., Ajdari, A., *Biopolymers* 1996, *39*, 755–759.

